

The Determination of the Rotational State and Interior Structure of Venus with VERITAS

G. Cascioli¹, S. Hensley², F. De Marchi¹, D. Breuer³, D. Durante¹, P. Racioppa¹, L. Iess¹, E. Mazarico⁴ and S. E. Smrekar²

¹Department of Mechanical and Aerospace Engineering, Sapienza University of Rome, Rome, Italy.

²Jet Propulsion Laboratory, California Institute of Technology, Pasadena, CA, USA.

³Institute for Planetary Research, German Aerospace Center (DLR), Berlin, Germany.

⁴NASA Goddard Space Flight Center, Greenbelt, MD, USA

Corresponding author: Gael Cascioli (gael.cascioli@uniroma1.it)

Key Points:

- The proposed VERITAS mission to Venus can provide unprecedented measurements of the planet's tidal response and rotational state
- The combined analysis of gravity science and synthetic aperture radar datasets can greatly benefit the scientific return of the mission
- VERITAS mission would allow to place tight constraints on the size and state of the core and on the viscous response of Venus.

Abstract

Understanding the processes that led Venus to its current state and will drive its future evolution is one of the main challenges of the next generation of space missions. In this work we analyze the retrieval of the spin vector, the tidal response and the moment of inertia of Venus with VERITAS, a Discovery-class mission proposed to NASA. By simulating the joint analysis of Doppler tracking data and tie points provided by the onboard synthetic aperture radar, we show that VERITAS would provide strong constraints on the interior structure of the planet. In particular we show that VERITAS would provide accuracies in the estimates of the tidal Love number k_2 to 3.9×10^{-4} , its tidal phase lag to 0.04° , and the moment of inertia factor to 1.4×10^{-3} (0.4% of the expected value).

Plain Language Summary

Understanding the processes that led Venus to its current state and will drive its future evolution is one of the main challenges of the next generation of space missions. VERITAS is a Discovery-class mission to Venus proposed to NASA which may be selected in the spring of 2021. In this work we simulate and analyze the capability of VERITAS of measuring geophysical parameters that are crucial to shed light on many open questions about our neighboring planet. We show that the measurements VERITAS will gather, would provide strong and new evidences about the interior structure of the planet and determine the state of the core (solid/liquid) its composition and the viscosity and composition of the mantle.

1 Introduction

The most comprehensive mapping of Venus was done by the Magellan mission in the early 1990s (Saunders et al., 1992). To succeed in its scope, Magellan employed a combination of Doppler tracking data and S-band Synthetic Aperture Radar (SAR), altimeter and radiometer to make nearly global observations of the surface of Venus (Ford & Pettengill, 1992). Magellan in-situ observations led to the most accurate estimate of the planet's spin axis orientation and sidereal rotation period (Davies et al., 1992, see also Campbell et al., 2019 for a resume of several observation campaigns), gravity field and tidal response (Konopliv et al., 1999; Konopliv & Yoder, 1996). The Magellan estimates, however, proved not sufficiently precise to constrain the interior structure. As shown in Dumoulin et al., (2017), current estimates of the tidal response do not distinguish between a liquid and solid core and the absence of a measurement of the tidal phase lag prevents from inferring the viscous response of the interior. Moreover, without direct observations of the moment of inertia factor ($\text{MOIF} = C/MR^2$ where C is the polar moment of inertia and M, R the planetary mass and radius, respectively), no constraints can be placed on the internal density profile and core size. Thus, models of Venus' interior rely on scaling Earth's interior structure to Venus' radius (e.g., Yoder, 1995; Aitta, 2012).

The Venus Emissivity, Radio science, INSAR, Topography And Spectroscopy (VERITAS) mission (Smrekar et al., 2021; Freeman et al., 2015) is a partnership led by NASA/JPL between US scientists and engineers, with strong collaborations and contributions of the German, Italian and French Space Agencies. It is one of four candidate NASA Discovery 2019 missions selected for a Concept Study Phase, expected to lead to a selection by NASA in the spring of 2021.

Among the main scientific objectives of VERITAS, the determination of the tidal response, tidal phase lag and MOIF are specifically focused at pushing forward our understanding of the Venus interior. VERITAS would carry two science instruments: VISAR (Venus Interferometric Synthetic Aperture Radar), the X-band interferometric radar (Hensley et al., 2020); and VEM, an infrared spectroscopic mapper (Helbert et al., 2020). Data from VISAR would be combined with two-way dual X- and Ka-band Doppler tracking data provided by the onboard telecom subsystem and used to improve estimates of the Love number k_2 , the tidal phase lag δ_{k_2} and the MOIF in order to constrain the structure of the Venus interior.

Arriving at Venus after a 9-month cruise, VERITAS would begin an 11-month aerobraking phase, paused after 5 months for 5 months of VEM science observations, before continuing to its final nearly circular polar orbit (180 x 255 km in altitude). VERITAS plans to operate for 4 Venus sidereal days (or 4 cycles, 243 Earth days each), providing a nearly global coverage of the planet for all its investigations (gravity science, VISAR, and VEM).

The goal of this work is to simulate the operational scenario of VERITAS' gravity experiment to assess the accuracy in the estimate of k_2 , δ_{k_2} and MOIF. This paper is structured as follows: in section 2 we describe the concept and the assumptions used in our simulations for both Doppler and radar measurements (sec 2.1 and 2.2 respectively); in section 3.1 we detail the methodology for the estimation of the MOIF, and discuss the simulation setup and observational scenario in section 3.2; in section 4 we present and discuss the results of the simulations; section 5 follows with concluding remarks.

2 Methods

It is well known that the sole knowledge of the gravitational field is not enough to infer the moments of inertia of a planet, which provide crucial constraints on its interior structure. To constrain the inertia tensor of a body, the gravity field information must be complemented by measurements of the rotational state. Precise Doppler tracking data, the primary observable quantity for gravity field recovery, are quite sensitive to the rotational state of the planet, but the attainable accuracy can be improved by augmenting the analysis with surface feature tracking. The latter provides direct observations of the rotational motion of the planet by measuring the inertial displacement of physical features located on the planet's surface. In this work, we make use of a combined processing of Earth-spacecraft Doppler tracking data and repeated surface landmark observations (tie points) provided by the onboard interferometric SAR.

2.1 Spacecraft Doppler Tracking

Doppler measurements are the primary observables for reconstructing the orbit of the spacecraft and recovering the gravity field of a planet. These measurements are collected by recording the Doppler shift of a radio signal sent from the ground station to the spacecraft, which then coherently retransmits it back to the Earth by means of an onboard transponder (two-way configuration). VERITAS' Doppler tracking system, with its heritage from ESA's BepiColombo (Iess et al., 2009, Iess et al., 2021), is able to establish two simultaneous coherent radio links in the X and Ka bands and to provide measurements of the range-rate of the probe with an accuracy of 0.018 mm/s (Ka band, 10s integration time) under nominal operational conditions (Cappuccio et al., 2020). The dual band configuration can be used near superior solar conjunctions to suppress

about 75% of the noise due to charged particles in the solar corona (Bertotti et al., 1993). In addition, the tracking system is capable of range measurements at the level of 2-3 cm at Ka band.

The operational scenario of VERITAS consists of five to seven Doppler tracking passes a week, collected by NASA's Deep Space Network ground stations. The VERITAS observation schedule entails approximately a daily contact to ground for 8 hours, and 16 hours of VISAR observations. For the gravity experiment we simulate 8-hour passes for five days a week collected by DSS 25 (Goldstone, CA), a station of the NASA Deep Space Network, with a white gaussian noise with standard deviation of 0.018 mm/s, removing data having an elevation angle below 15° and accounting for occultation periods. The integration time of synthetic Doppler observables is set to 10 s, which is sufficient to resolve gravity field features as small as 190 km after 4 cycles.

2.2 Radar Observations and Tie Points

The VERITAS orbit is designed to have overlapping ground tracks from cycle to cycle to enable repeating passes for radar interferometric observations. Radar data are collected on 11 out of 16 orbits per day, and downlinked to Earth on the remaining 5 orbits, when two-way X and Ka band tracking data are acquired. Therefore, radar and Doppler data are not collected simultaneously.

VISAR is an X-band interferometric radar operating at 7.9 GHz (3.8 cm wavelength) and has a 20 MHz bandwidth from which radar imagery with 30 m ground resolution pixels and topographic data with 250 m spatial resolution and ~ 5 m elevation accuracy is produced. The radar acquires data with a look angle of 30° (angle between the antenna boresight and spacecraft nadir) and images a swath width of 14.4 km (Figure 1). After an orbital period, planetary rotation shifts the VERITAS ground tracks by roughly 10 km; thus, the swath width provides more than 2 km of overlap between swaths acquired on adjacent orbits, enabling coherent mapping of Venus surface.

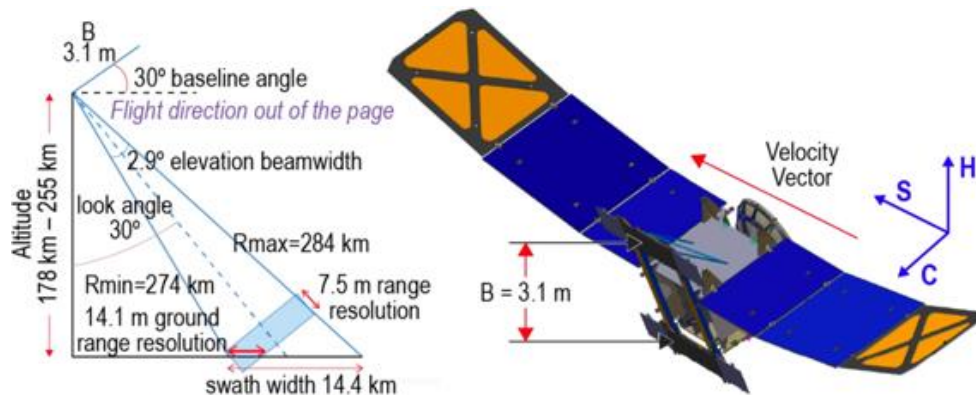


Figure 1. VISAR flight configuration and observing geometry.

VISAR transmits pulses and records the received echoes to generate images of the backscattered signal from the surface. To achieve fine resolution in the radar along-track or azimuth direction, SAR image formation combines echoes from multiple pulses when a point is illuminated by the radar antenna beam. The pixel location in a radar image is determined by the range, i.e., distance

from the platform to the pixel, and the Doppler frequency, i.e., projection of spacecraft velocity on the line-of-sight. For Venus, the range, derived from the delay between pulse transmit time and echo return time, must be corrected for the delay induced by the thick Venus atmosphere. Atmospheric contribution amounts to 200-400 m of additional range, depending on the pixel elevation and imaging geometry. Since VISAR is an interferometer, it solves for the 3-dimensional position of each pixel using the range, Doppler and interferometric phase from two spatially separated antennas. Surface features (landmarks) imaged on multiple orbits can be identified using automated matching software.

To include radar tie points in our simulations, we generated a simulated dataset of radar observations. Two classes of radar tie points were simulated. The first class of radar tie points (*local tie points*) are observed in the swath overlap region of adjacent orbits. These measurements would allow to better determine the trajectory of the probe by providing constraints between adjacent orbits when VERITAS is not tracked by the DSN. The second class of radar tie points are the so-called *global tie points*. A point on the surface can in principle be imaged up to 8 times (excluding swath overlaps) during the 4-cycle mission: one time each on the descending and ascending passes, for each of the four cycles. Each observation is separated by half a Venus sidereal period thus enabling to place tight constraints on the inertial motion of surface features, directly related to the rotational state of the planet.

For the simulation, we placed global tie points on a latitude/longitude grid with approximately 150 km spacing separating points in both directions. We exclude orbits that are used for data downlink, in solar conjunction or in power-restricted orbits where data is not collected. The relative range and Doppler measurement errors depend on how accurately imagery acquired from different orbits can be matched. SAR image matching is hindered by speckle that results in a grainy appearance due to the coherent nature of imaging and from differences in imaging geometry, either incidence angle or look direction. Matching accuracy is a function of the image signal-to-noise ratio, the number of looks used to reduce both speckle and thermal noise, imaging geometry differences and the amount of scene contrast (see section S4).

Identification of radar tie points would use an automated scene matching algorithm. The automated matching algorithm computes the cross correlation for a search window that covers the largest expected offset due to ephemeris errors.

To account for the spatially variable nature of the matching accuracy, and the consequent range and Doppler measurement error, we adopt the match covariance matrix used in the automated matching algorithm to estimate the matching accuracy (Frankot et al., 1994). We tune the matching metric based on match accuracy statistics from Magellan stereo data that covered approximately 20% of the surface (for additional details see section S4).

The average accuracy of the range and Doppler observations of each radar tie point is 3 m and 10 Hz derived from an average 0.2 pixel matching accuracy using a 64×64 matching window of 30

m resolution pixel imagery where each pixel corresponds to 15 m of range and 40 Hz of Doppler. A total of 710,496 tie points were simulated corresponding to 43,980 unique landmarks.

3 Numerical Simuations

3.1 Determination of the Moment of Inertia from the Rotational State

The torque of the Sun on Venus determines the precession of its spin axis in a conical motion about the orbit normal. The precession rate Ω is:

$$\Omega = \frac{3}{2} \frac{n^2}{\omega} \cos \epsilon \frac{J_2}{k} \quad (1)$$

where J_2 is the un-normalized degree 2 zonal coefficient of the gravity field of Venus, k is the MOIF, ω is the sidereal spin rate, n is the mean motion and ϵ the obliquity (angle between spin axis and orbit normal). If a measurement of the precession rate of the spin axis is available, Equation (1) can be used to estimate the MOIF of the planet. The precession of Venus, deduced from Equation (1), has a period of ~ 29.000 yr (Cottureau & Souchay, 2009) for reasonable ranges of MOIF values. Although Ω is relatively large (during the 4 Venus cycles spanned by VERITAS the angular displacement of the pole is about 0.03°) relative to the small axial tilt of the planet (2.64°), the physical displacement of the pole on Venus surface corresponds to only 151 m. Note that the attainable accuracy on the MOIF primarily results from the accuracy of the precession rate, since J_2 and the other quantities in Eq. (1) are much better known.

As the precession period is much longer than the VERITAS observations, the precessional motion of Venus can be described by three first-degree polynomials for the spin vector right ascension, $\alpha(t) = \alpha_0 + \dot{\alpha}(t - t_0)$, declination $\delta(t) = \delta_0 + \dot{\delta}(t - t_0)$, and prime meridian, $w(t) = w_0 + \frac{2\pi(t-t_0)}{T_{sid}}$, with t_0 corresponding to the J2000 epoch and T_{sid} being the sidereal period (see e.g., Archinal et al. 2009). The precession constant Ω can be directly associated (under the assumption of negligible nutations and small deviation from the reference position, as shown in the supporting information S3) to $\dot{\alpha}$ and $\dot{\delta}$ as:

$$\Omega = c_1 \dot{\alpha} = c_2 \dot{\delta} \quad (2)$$

with the coefficients c_1 and c_2 determined by the orbital inclination of Venus, the reference position of the pole (α_0, δ_0) and the longitude of the orbital node at the reference epoch. In our simulations we therefore estimate the pole polynomial coefficients and exploit the aforementioned procedure to assess the uncertainty on Ω and thus on the MOIF.

To verify the validity of our approach, we have developed a more detailed (and computationally expensive) model of Venus's rotational state, based on the numerical integration of the Euler equations for the rigid body, taking into account the gravitational torques exerted on Venus by all the main solar system bodies. This model directly embeds the dependence from the inertia tensor and its relationship with gravity field quadrupole coefficients (via the McCullagh formula; Murray & Dermott, 2000), yielding a direct estimate of the MOIF. We verified that the results

obtained under the linear assumption are in very good agreement with the numerically integrated model and thus opted for the former for the sake of reducing the computational effort.

3.2 Simulation Setup and Scenario

To assess the capabilities of VERITAS to retrieve the rotational state, Love numbers and MOIF we conducted an extensive set of numerical simulations replicating the nominal operational scenario of VERITAS.

We randomly downsampled the full set of simulated landmarks to ~8000. The choice of simulating only a subset of landmarks is supported by two arguments. Firstly, observations of a landmark-dense area might be highly correlated. Selecting only well-spaced points justifies the assumption that the observations are statistically independent, therefore simplifying the analysis. Secondly, the outcome of the simulation can be considered as a conservative estimate of what would be possible if the entire dataset is processed (for a discussion on the influence of the number of measured landmarks refer to the supporting information S1).

We assessed the capabilities of VERITAS through a covariance analysis. Using the JPL orbit determination software MONTE (Evans et al., 2018), we integrate the trajectory of the probe, generate synthetic Doppler and VISAR data according to the assumptions outlined in Sec. 2.1 and 2.2, add white gaussian noise (according to the expected noise levels, 0.018 mm/s for Earth-spacecraft Doppler tracking and 3m and 10Hz for the radar tie points in range and Doppler respectively) and combine all the data in a least squares filter (ORACLE) developed at Sapienza University and validated with several space missions (e.g., Iess et al., 2018). The practical implementation of the combined processing procedure is straightforward. The tie points measurements, being in the form of range and range-rate do not require special handling and can be directly used in the orbit determination least squares batch filter. We used this estimation technique, together with the multiarc approach that is best suited for data analysis of long duration gravity experiments (e.g., Durante et al., 2020; Mazarico et al., 2014; Konopliv et al., 2013).

The dynamical model used to propagate the spacecraft trajectory includes the monopole gravitational acceleration of all main solar system bodies, a degree and order 50 static gravity field of Venus (derived from Konopliv et al., 1999 - we limit the spherical expansion to degree 50 since higher degrees have negligible effects on the results for the parameters of interest), the tidal response to the Sun and the atmospheric thermal tides, the non-gravitational accelerations due to solar radiation pressure and atmospheric drag. Density variations, depending on local time and solar activity (Müller-Wodarg et al., 2016, Kliore et al., 1992), induce accelerations on the spacecraft over typical time scales ranging from half to a quarter of the orbital period. It is a common procedure for the orbit determination of orbiters around thick-atmosphere planets to account for the unpredictable short-term variability of the drag acceleration by modeling the drag coefficient C_d as a time-varying parameter with time update depending on the time scale of the atmospheric phenomena. In our simulations we chose to model a time-varying C_d by estimating a set of piece-wise constant along-track accelerations with a time update of 30 minutes.

Our model includes also atmospheric thermal tides as the spacecraft tracking system will be sensitive to their effect (Goossens et al., 2018, Bills et al., 2020). The numerical results we report

in the next paragraphs are based on the assumption of a knowledge of the atmospheric pressure model with an initial 10% accuracy. Thermal tides modeling and the effect of the assumed a priori knowledge on the final results is discussed in S2.

We run the described filter solving for the set of parameters of interest. In our multiarc approach, the tracking data are subdivided in 2.5-day arcs and the parameters are divided in two sets: local parameters (those affecting a single arc, e.g. position and velocity of the probe) and global parameters (parameters affecting all the arcs, e.g. the gravity field of the planet). The complete list of parameters comprises the state of the probe, empirical along-track accelerations, Venus gravity field spherical harmonics coefficients up to degree and order 50, complex Love number of degree 2, the Venus pole location (right ascension, declination) and its precession rate, the Venus sidereal period, the thermal tide-induced gravity field correction coefficients (as detailed in S2) and the coordinates of each of the observed landmarks (latitude, longitude, altitude), for a total of 27,320 global parameters.

4 Results and Discussion

Table 1 reports the uncertainties (all results in tables and text, unless otherwise stated, are three times the formal uncertainty) attainable for the Venus rotational parameters, the Love number and the MOIF in the nominal VERITAS mission configuration in two cases: Doppler tracking data only, and Doppler tracking data combined with VISAR observations. The inclusion of VISAR tie point measurements in the orbit determination enables a large improvement in the determination of the rotational state of Venus, not attainable with Doppler data alone. The tie points increase the accuracy in the pole location and MOIF by about a factor of 6, while a smaller improvement (~ 2.5) is found on k_2 and its tidal phase lag.

The current estimate of Venus Love number (0.295 ± 0.066 , 2σ , Konopliv & Yoder 1996), coupled with the lack of a magnetic field, does not allow resolving between a liquid and solid core (Dumoulin et al., 2017, see figure 2). Dumoulin et al. (2017) determined that the state of the core and its size, as well as the viscous response of the interior, can be well constrained with a knowledge of k_2 to an accuracy smaller than 3% (0.01) and phase lag $\sigma_{\delta_{k_2}} < 0.25^\circ$.

Our simulations show that VERITAS will be able to determine these tidal quantities with an accuracy substantially better than these threshold values. Right ascension and declination of the pole (α_0 and δ_0) can be determined with an accuracy increased by an average factor of 6, improving the results obtained by Magellan by more than 100 times. A comparable improvement is found for the obliquity ϵ ($\sigma_\epsilon = 160 \text{ mas}$). VERITAS will also enable the determination of the precession rate Ω to a level of $5.1 \times 10^{-3} \text{ deg/century}$, which allows the retrieval of the MOIF (with the procedure and constraint detailed in Sec 3.1 and S3). This would be the first dynamical measurement of Venus MOIF resulting in an accuracy of 0.4% of its predicted central value (0.336, Cottureau & Souchay, 2009). The accurate measurement of the MOIF provides an

additional, strong constraint to improved models of the Venus interior, by reducing the uncertainty in the density of the core and the mantle.

Based on current models (Dumoulin et al., 2017) the constraints on k_2 and δ_{k_2} can determine core state, and core size to within 100 km and average mantle viscosity to within an order of magnitude (See Figure 2). The latter value strongly depends on the temperature distribution and the volatile content in the mantle and therefore provides information about the heat and volatile loss of the planet. For example, a warm and wet mantle, representative of a planetary interior that has not cooled much and has lost little of its original water, has a low viscosity, while a cold and dry mantle, representative of an efficiently cooled and outgassed interior, has a high viscosity. These two extreme models would differ in viscosity by several orders of magnitude and could be distinguished in measuring the phase lag.

Different formation scenarios lead to different compositional models based on cosmochemical assumptions and trends among Earth-like planets to model the interior of Venus. A major difference in the models is the FeO content of the mantle, which can vary between 0.42 and 18.7 wt. %. This results in different values of MOIF ranging between 0.33 and 0.342 (~3 % variation), with otherwise the same assumption about the thermal state and the core composition (Dumoulin et al., 2017). Knowledge of the MOIF with an accuracy of 0.4% will therefore further help to distinguish the mantle composition models.

The amount of light elements in the core, particularly important for a better understanding of Venus' magnetic field evolution and also informative about Venus' conditions during core formation, is not known. The two parameters together, k_2 and MOIF, help to better distinguish the models as has already been shown, for example, for Mars (Rivoldini et al. 2011). The information about the density distribution from the MOIF is not unique, i.e. for the same MOIF the core can be small and dense or relatively larger and lighter. If the core of Venus is liquid, the core size can be constrained independently with k_2 and thus in combination of MOIF also the core density.

All these fundamental quantities, such as core state, size and composition, mantle composition and viscosity, are necessary to understand the formation of Venus and its thermal and magnetic evolution. They serve, for example, as inputs (core radius and core and mantle composition) or constraints (core state and present effective mantle viscosity) for modelling core and mantle processes and the thermal and magnetic evolution.

VERITAS would also provide a tight constraint on the sidereal rotation period of Venus (T_{sid}) at the sub-second level ($\sigma_{T_{sid}} = 0.13$ s).

As a by-product of the estimation process, we can determine the location of all observed landmarks, thus providing the backbone of an accurate geodetic control network. The median values of the recovered landmark position accuracy in altitude, latitude and longitude (mapped on the reference surface of Venus) are respectively $M_{alt} = 3$ m, $M_{lat} = 9$ m, $M_{lon} = 12.6$ m. The determination of the landmark positions allows also to retrieve the radial displacement associated to the tidal forcing, parametrized by the Love number h_2 . The retrieved uncertainty

($\sigma_{h_2} = 0.195$, corresponding to ~ 12 cm of maximum radial displacement) allows to determine h_2 to 25-45% of its predicted value (0.45-0.75 Dumoulin et al., 2017).

The inclusion of tie points improves the orbital solution by providing observability during periods in which the spacecraft is not tracked from the Earth. This aspect is particularly important for providing a uniform tracking coverage along the orbit and giving robustness to the determination of physical effects such as atmospheric drag whose variability cannot be predicted with enough accuracy by a deterministic a priori model. The denser availability of orbit-related data is also the reason for a slight enhancement of the low-degree gravity field retrieval, since it allows a better resolution of the large spatial scales (i.e., low degree) of the planetary gravitational field. The improvement of the static gravity field determination is strictly related to the improvement of the (complex) Love number.

Table 1 Results of the numerical simulations. We report the uncertainties in the two cases of Doppler only and Doppler + Tie points analyses (three times the formal uncertainty). The tie points improvement factor is the ratio between the uncertainties obtained without and with the inclusion of VISAR data.

Parameter	Current uncertainty from observations	Source	Earth Doppler Only	Earth Doppler + Tie Points	Tie Points Improvement Factor
α_0 [arcsec]	72	Davies et al., 1992	2.3	0.36	6.3
δ_0 [arcsec]	36		1.3	0.21	6.2
T_{sid} [day]	1×10^{-4}		1.1×10^{-5}	1.5×10^{-6}	7.1
ϵ [arcsec]	30	Derived from Davies et al., 1992	1.0	0.16	6.3
Ω [deg/century]	-	-	3.2×10^{-2}	5.1×10^{-3}	6.3
$MOIF$	-	-	8.6×10^{-3}	1.4×10^{-3}	6.3
k_2	6.6×10^{-2}	Konopliv and Yoder, 1996	9.6×10^{-4}	3.9×10^{-4}	2.5
δ_{k_2} [deg]	-	-	8.6×10^{-2}	4.0×10^{-2}	2.1

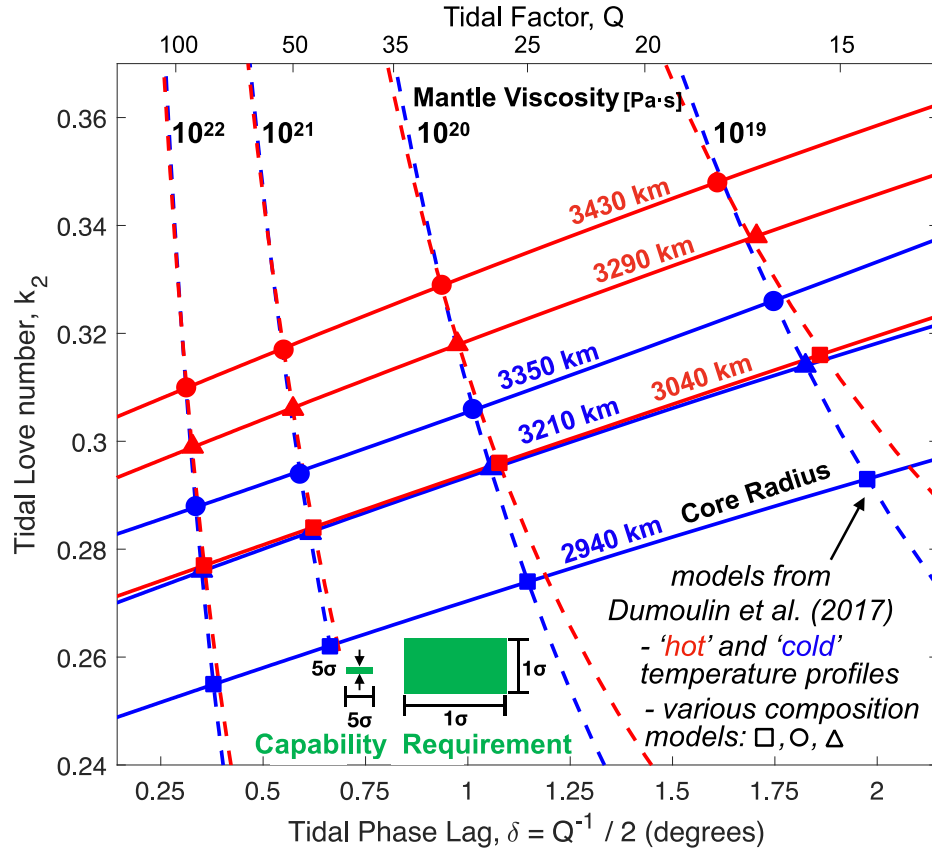


Figure 2 The required uncertainty on Love number k_2 and the tidal phase lag to constrain core radius and mantle viscosity according to Dumoulin et al., 2017 (right green box) is compared with the experiment capability (left green box, here shown at 5 times the formal uncertainty) showing the possibility to constrain the interior structure of Venus to unprecedented accuracy.

5 Conclusions

By simulating the nominal mission scenario of the proposed VERITAS mission to Venus, we showed that VERITAS will be able to determine with very good accuracy the physical parameters needed to build a detailed understanding of the planet's interior structure. The precise characterization of the tidal response of Venus via the measurement of its complex Love number will allow to place tight constraints on the state of the core and on the viscous response of the planet. The combined processing of Earth Doppler tracking and VISAR data proves to be extremely effective in the determination of the rotational state of the planet and the moment of inertia factor, further extending the possibility of understanding of the dynamical evolution of Earth's neighboring planet. These fundamental quantities, which are little known so far, are necessary to understand the formation of Venus and its thermal and magnetic evolution - also in the context of the other terrestrial planets. Ultimately they can provide valuable clues as to how and why Venus evolved into an uninhabitable planet.

Acknowledgments, Samples, and Data

The work of G.C, F.D.M, P.R., D.D and L.I. has been supported by the Italian Space Agency (ASI) contract 2020-15-HH.0.

A portion of this research was conducted at the Jet Propulsion Laboratory, California Institute of Technology, under contract with the National Aeronautics and Space Administration. The information presented about VERITAS is pre-decisional and is provided for planning and discussion purposes only.

Data were not used, nor created for this research.

References

- Saunders, R. S., Spear, A. J., Allin, P. C., Austin, R. S., Berman, A. L., Chandler, R. C., Clark, J., Decharon, A. V., De Jong, E. M., Griffith, D. G., Gunn, J. M., Hensley, S., Johnson, W. T. K., Kirby, C. E., Leung, K. S., Lyons, D. T., Michaels, G. A., Miller, J., Morris, R. B., ... Wall, S. D. (1992). Magellan mission summary. *Journal of Geophysical Research*, 97(E8), 13067. <https://doi.org/10.1029/92JE01397>
- Ford, P. G., & Pettengill, G. H. (1992). Venus topography and kilometer-scale slopes. *Journal of Geophysical Research*, 97(E8), 13103. <https://doi.org/10.1029/92JE01085>
- Campbell, B. A., Campbell, D. B., Carter, L. M., Chandler, J. F., Giorgini, J. D., Margot, J. L., Morgan, G. A., Nolan, M. C., Perillat, P. J., & Whitten, J. L. (2019). The mean rotation rate of Venus from 29 years of Earth-based radar observations. *Icarus*. <https://doi.org/10.1016/j.icarus.2019.06.019>
- Hensley, S., Campbell, B., Perkovic-Martin, D., Wheeler, K., Kiefer, W., Ghail, R. (2020) "VISAR and VenSAR: Two Proposed Radar Investigations of Venus," *IEEE Radar Conference (RadarConf20)*, Florence, Italy, 2020, <http://10.1109/RadarConf2043947.2020.9266323>
- Aitta, A. (2012). Venus' internal structure, temperature and core composition. *Icarus*, 218(2), 967–974. <https://doi.org/10.1016/j.icarus.2012.01.007>
- Yoder, C. F. (1995). Venus' Free Obliquity. *Icarus*, 117(2), 250–286. <https://doi.org/10.1006/icar.1995.1156>
- Helbert, J., Säuberlich, T., Dyar, M. D., Ryan, C., Walter, I., Réess, J.-M., et al. (2020). The Venus Emissivity Mapper (VEM): advanced development status and performance evaluation. In M. Strojnik (Ed.), *Infrared Remote Sensing and Instrumentation XXVIII* (p. 6). SPIE. <https://doi.org/10.1117/12.2567634>
- Cappuccio, P., Notaro, V., Di Ruscio, A., Iess, L., Genova, A., Durante, D., et al. (2020). Report on first inflight data of BepiColombo's Mercury Orbiter Radio-science Experiment. *IEEE*

Transactions on Aerospace and Electronic Systems, 1–1.

<https://doi.org/10.1109/TAES.2020.3008577>

Bertotti, B., Comoretto, G., & Iess, L. (1993). Doppler tracking of spacecraft with multi-frequency links. *Astronomy and Astrophysics*, 269(1–2), 608–616.

Iess, L., Folkner, W. M., Durante, D., Parisi, M., Kaspi, Y., Galanti, E., et al. (2018). Measurement of Jupiter’s asymmetric gravity field. *Nature*, 555(7695), 220–222.

<https://doi.org/10.1038/nature25776>

Durante, D., Parisi, M., Serra, D., Zannoni, M., Notaro, V., Racioppa, P., et al. (2020). Jupiter’s Gravity Field Halfway Through the Juno Mission. *Geophysical Research Letters*, 47(4).

<https://doi.org/10.1029/2019GL086572>

Mazarico, E., Genova, A., Goossens, S., Lemoine, F. G., Neumann, G. A., Zuber, M. T., Smith, D. E., & Solomon, S. C. (2014). The gravity field, orientation, and ephemeris of Mercury from MESSENGER observations after three years in orbit. *Journal of Geophysical Research: Planets*, 119(12), 2417–2436.

<https://doi.org/10.1002/2014JE004675>

Konopliv, A. S., Park, R. S., Yuan, D.-N., Asmar, S. W., Watkins, M. M., Williams, J. G., Fahnestock, E., Kruizinga, G., Paik, M., Strelakov, D., Harvey, N., Smith, D. E., & Zuber, M. T. (2013). The JPL lunar gravity field to spherical harmonic degree 660 from the GRAIL Primary Mission. *Journal of Geophysical Research: Planets*, 118(7), 1415–1434.

<https://doi.org/10.1002/jgre.20097>

Konopliv, A. S., Banerdt, W. B., & Sjogren, W. L. (1999). Venus Gravity: 180th Degree and Order Model. *Icarus*, 139(1), 3–18.

<https://doi.org/10.1006/icar.1999.6086>

Konopliv, A. S., & Yoder, C. F. (1996). Venusian k₂ tidal Love number from Magellan and PVO tracking data. *Geophysical Research Letters*, 23(14), 1857–1860.

<https://doi.org/10.1029/96GL01589>

Müller-Wodarg, I. C. F., Bruinsma, S., Marty, J.-C., & Svedhem, H. (2016). In situ observations of waves in Venus’s polar lower thermosphere with Venus Express aerobraking. *Nature Physics*, 12(8), 767–771.

<https://doi.org/10.1038/nphys3733>

Kliore, A. J., Keating, G. M., & Moroz, V. I. (1992). Venus international reference atmosphere (1985). *Planetary and Space Science*, 40(4), 573.

[https://doi.org/10.1016/0032-0633\(92\)90255-M](https://doi.org/10.1016/0032-0633(92)90255-M)

Bills, B. G., Navarro, T., Schubert, G., Ermakov, A., & Górski, K. M. (2020). Gravitational signatures of atmospheric thermal tides on Venus. *Icarus*, 340, 113568.

<https://doi.org/10.1016/j.icarus.2019.113568>

- 431 Cottureau, L., & Souchay, J. (2009). Rotation of rigid Venus: a complete precession-nutation
432 model. *Astronomy & Astrophysics*, 507(3), 1635–1648. [https://doi.org/10.1051/0004-
433 6361/200912174](https://doi.org/10.1051/0004-6361/200912174)
- 434 Dumoulin, C., Tobie, G., Verhoeven, O., Rosenblatt, P., & Rambaux, N. (2017). Tidal
435 constraints on the interior of Venus. *Journal of Geophysical Research: Planets*, 122(6),
436 1338–1352. <https://doi.org/10.1002/2016JE005249>
- 437 Genova, A., Goossens, S., Lemoine, F. G., Mazarico, E., Neumann, G. A., Smith, D. E., &
438 Zuber, M. T. (2016). Seasonal and static gravity field of Mars from MGS, Mars Odyssey
439 and MRO radio science. *Icarus*, 272, 228–245. <https://doi.org/10.1016/j.icarus.2016.02.050>
- 440 Frankot, R. T., Hensley, S., & Shafer, S. (1994). Noise resistant estimation techniques for SAR
441 image registration and stereo matching. In *Proceedings of IGARSS '94 - 1994 IEEE
442 International Geoscience and Remote Sensing Symposium* (Vol. 2, pp. 1151–1153). IEEE.
443 <https://doi.org/10.1109/IGARSS.1994.399369>
- 444 Davies, M. E., Colvin, T. R., Rogers, P. G., Chodas, P. W., Sjogren, W. L., Akim, E. L., et al.
445 (1992). The rotation period, direction of the North Pole, and geodetic control network of
446 Venus. *Journal of Geophysical Research*, 97(E8), 13141.
447 <https://doi.org/10.1029/92JE01166>
- 448 Iess, L., Asmar, S.W., Cappuccio, P. et al. Gravity, Geodesy and Fundamental Physics with
449 BepiColombo's MORE Investigation. *Space Science Reviews* 217, 21 (2021).
450 <https://doi.org/10.1007/s11214-021-00800-3>
- 451 Iess, L., Asmar, S., & Tortora, P. (2009). MORE: An advanced tracking experiment for the
452 exploration of Mercury with the mission BepiColombo. *Acta Astronautica*.
453 <https://doi.org/10.1016/j.actaastro.2009.01.049>
- 454 Evans, S., Taber, W., Drain, T., Smith, J., Wu, H.-C., Guevara, M., et al. (2018). MONTE: the
455 next generation of mission design and navigation software. *CEAS Space Journal*, 10(1), 79–
456 86. <https://doi.org/10.1007/s12567-017-0171-7>
- 457 Archinal, B. A., A'Hearn, M. F., Bowell, E., Conrad, A., Consolmagno, G. J., Courtin, R., ...
458 Williams, I. P. (2011). Report of the IAU Working Group on Cartographic Coordinates and
459 Rotational Elements: 2009. *Celestial Mechanics and Dynamical Astronomy*, 109(2), 101–
460 135. <https://doi.org/10.1007/s10569-010-9320-4>
- 461 Murray, C. D., & Dermott, S. F. (2000). Solar System Dynamics. In *Solar System Dynamics*.
462 Cambridge University Press. <https://doi.org/10.1017/CBO9781139174817>
- 463 Simon, J. L., Bretagnon, P., Chapront, J., Chapront-Touze, M., Francou, G., Laskar, J. (1994).
464 Numerical expressions for precession formulae and mean elements for the Moon and the planets.
465 *Astron. Astrophys.* 282, 663–683 . <https://ui.adsabs.harvard.edu/abs/1994A&A...282..663S>

Smrekar, S. and the VERITAS science team, VERITAS (Venus Emissivity, Radio Science, INSAR, Topography And Spectroscopy): A Proposed Discovery Mission, Lunar Plan. Sci. Conf, Abstract #, 2021.

Garate-Lopez, I., & Lebonnois, S. (2018). Latitudinal variation of clouds' structure responsible for Venus' cold collar. *Icarus*. <https://doi.org/10.1016/j.icarus.2018.05.011>

Freeman, A., & Smrekar, S. E. (2015). VERITAS – a Discovery-class Venus surface geology and geophysics mission. In *11th Low Cost Planetary Missions Conference*.

Goossens, S., Mazarico, E., Rosenblatt, P., Lebonnois, S., & Lemoine, F. (2018, November). Venus Gravity Field Determination Using Magellan and Venus Express Tracking Data. In *16th Meeting of the Venus Exploration and Analysis Group (VEXAG)* (Vol. 16, No. 2137, p. 8029).

Goossens, S., Lemoine, F. G., Rosenblatt, P., Lebonnois, S., & Mazarico, E. (2017, March). Venus Gravity Field Modeling from Magellan and Venus Express Tracking Data. In *Lunar and Planetary Science Conference* (No. 1964, p. 1984)

Petrov, L. (2004). Study of the atmospheric pressure loading signal in very long baseline interferometry observations. *Journal of Geophysical Research*, 109(B3), B03405. <https://doi.org/10.1029/2003JB002500>

Rivoldini, A., Van Hoolst, T., Verhoeven, O., Mocquet, A., & Dehant, V. (2011). Geodesy constraints on the interior structure and composition of Mars. *Icarus*, 213(2), 451–472. <https://doi.org/10.1016/j.icarus.2011.03.024>